

Strong near-field couplings of anapole modes and formation of higher-order electromagnetic modes in stacked all-dielectric nanodisks

Bin Liu(刘彬), Ma-Long Hu(胡马龙), Yi-Wen Zhang(章艺文), Yue You(游悦), Zhao-Guo Liang(梁钊国), Xiao-Niu Peng(彭小牛), and Zhong-Jian Yang(杨中见)

Citation: Chin. Phys. B, 2022, 31 (**5**): 057802. DOI: 10.1088/1674-1056/ac3bac
Journal homepage: http://cpb.iphy.ac.cn; http://iopscience.iop.org/cpb

What follows is a list of articles you may be interested in

Improving the performance of a GaAs nanowire photodetector using surface plasmon polaritons

Xiaotian Zhu(朱笑天), Bingheng Meng(孟兵恒), Dengkui Wang(王登魁), Xue Chen(陈雪), Lei Liao(廖蕾), Mingming Jiang(姜明明), and Zhipeng Wei(魏志鹏)

Chin. Phys. B, 2022, 31 (**4**): 047801. DOI: 10.1088/1674-1056/ac1e15

A theoretical study on chemical ordering of 38-atom trimetallic Pd-Ag-Pt nanoalloys

Songül Taran, Ali Kemal Garip, Haydar Arslan

Chin. Phys. B, 2020, 29 (**7**): 077801. DOI: 10.1088/1674-1056/ab99b4

Cascaded plasmonic nanorod antenna for large broadband local electric field enhancement

Dou Zhang(张豆), Zhong-Jian Yang(杨中见), Jun He(何军)

Chin. Phys. B, 2019, 28 (**10**): 107802. DOI: 10.1088/1674-1056/ab3f99

Hot spots enriched plasmonic nanostructure-induced random lasing of quantum dots thin film

Feng Shan(单锋), Xiao-Yang Zhang(张晓阳), Jing-Yuan Wu(吴静远), Tong Zhang(张彤)

Chin. Phys. B, 2018, 27 (**4**): 047804. DOI: 10.1088/1674-1056/27/4/047804

Shape controllable synthesis and enhanced upconversion photoluminescence of β-$NaGdF_4$:Yb^{3+}, Er^{3+} nanocrystals by introducing Mg^{2+}

Yong-Xin Yang(杨永馨), Zheng Xu(徐征), Su-Ling Zhao(赵谡玲), Zhi-Qin Liang(梁志琴), Wei Zhu(朱薇), Jun-Jie Zhang(张俊杰)

Chin. Phys. B, 2017, 26 (**8**): 087801. DOI: 10.1088/1674-1056/26/8/087801

Strong near-field couplings of anapole modes and formation of higher-order electromagnetic modes in stacked all-dielectric nanodisks

Bin Liu(刘彬)[1,2], Ma-Long Hu(胡马龙)[2], Yi-Wen Zhang(章艺文)[2], Yue You(游悦)[2], Zhao-Guo Liang(梁钊国)[1], Xiao-Niu Peng(彭小牛)[1,†], and Zhong-Jian Yang(杨中见)[2,‡]

[1] *Hubei Key Laboratory of Ferroelectric and Dielectric Materials and Devices, Faculty of Physics and Electronic Science, Hubei University, Wuhan* 430062, *China*

[2] *Hunan Key Laboratory of Nanophotonics and Devices, School of Physics and Electronics, Central South University, Changsha* 410083, *China*

(Received 29 September 2021; revised manuscript received 15 November 2021; accepted manuscript online 20 November 2021)

We theoretically study the near-field couplings of two stacked all-dielectric nanodisks, where each disk has an electric anapole mode consisting of an electric dipole mode and an electric toroidal dipole (ETD) mode. Strong bonding and anti-bonding hybridizations of the ETD modes of the two disks occur. The bonding hybridized ETD can interfere with the dimer's electric dipole mode and induce a new electric anapole mode. The anti-bonding hybridization of the ETD modes can induce a magnetic toroidal dipole (MTD) response in the disk dimer. The MTD and magnetic dipole resonances of the dimer form a magnetic anapole mode. Thus, two dips associated with the hybridized modes appear on the scattering spectrum of the dimer. Furthermore, the MTD mode is also accompanied by an electric toroidal quadrupole mode. The hybridizations of the ETD and the induced higher-order modes can be adjusted by varying the geometries of the disks. The strong anapole mode couplings and the corresponding rich higher-order mode responses in simple all-dielectric nanostructures can provide new opportunities for nanoscale optical manipulations.

Keywords: all-dielectric nanodisks, anapole, electric toroidal dipole, magnetic toroidal dipole

PACS: 78.67.Bf, 42.25.Fx **DOI:** 10.1088/1674-1056/ac3bac

1. Introduction

Much progress has recently been made in nanophotonics research and development with applications in metasurfaces,[1,2] nonlinear optics,[3,4] and nano-antennas.[5,6] Plasmonic nanostructures have played an essential part in these sub-fields. Plasmonic nanostructures mainly support electric dipole (ED) and electric multipole modes.[7] However, the material losses of plasmonic structures are usually high. Recently, all-dielectric nanostructures with low material loss have become another important branch of nanophotonics.[8,9] In all-dielectric nanostructures, electric and magnetic resonance modes can be readily excited in simple structures. These electromagnetic resonances of dielectric structures are of fundamental importance for their applications. The typical electric and magnetic dipole or higher-order modes can further interact, providing new routes to adjust the optical responses of dielectric nanostructures. Many relevant optical phenomena have been reported, including the electric/magnetic dipole mode hybridization[10] and Fano resonance.[11–13]

In addition to the standard dipole and multipole electromagnetic modes, nonradiating electromagnetic states in all-dielectric nanostructures have recently attracted many research interests.[14–18] These new nanophotonic modes include anapole modes, where an electric anapole is induced by the coherent combination of an electric dipole and an electric toroidal dipole (TD) moment.[15] An ETD mode can be regarded as a higher-order term of the electric dipole expression in the Cartesian multipole decomposition method.[19–21] The toroidal multipole and the electric dipole have the same radiation pattern, but their current configurations are different. The electric anapole has been widely investigated in many aspects of nanophotonics, such as local field enhancement,[22–25] nonlinear optical effects,[26–29] photon–exciton coupling,[30,31] hybrid dielectric-plasmonic antennas,[32–34] and metamaterials.[35] Similar to the ETD mode, the magnetic toroidal dipole (MTD) has also been studied. MTD can be formed by a closed loop of the ETD moments.[20,36–38] MTD and the magnetic dipole (MD) can form a magnetic anapole mode.

Here, we show that the electric anapole modes can be strongly coupled through nearfield interactions. The structure consists of stacked all-dielectric nanodisks, where the two silicon (Si) nanodisks are the same. The ETD modes of the anapoles of the two disks can form bonding and anti-bonding hybridized modes. A new electric anapole mode of the whole dimer is found due to the interference between the bonding hybridized ETD and ED modes. It is also found that the anti-bonding hybridization of the ETD modes can induce an MTD response of the disk dimer. The MTD and MD resonances of the dimer will lead to a magnetic anapole mode. Thus, two dips associated with the hybridized modes appear on the

†Corresponding author. E-mail: pengxn@hubu.edu.cn
‡Corresponding author. E-mail: zjyang@csu.edu.cn

© 2022 Chinese Physical Society and IOP Publishing Ltd

scattering spectrum of the dimer. The MTD resonance is also accompanied by the electric toroidal quadruple (ETQ) mode. Multipole expansions and near-field distributions will be calculated to identify the higher-order electromagnetic mode responses. The hybridizations of the ETDs and the formatted higher-order modes can be tuned by varying the geometries of the disks.

2. Results and discussion

Figure 1(a) shows the structure's schematic, where the polarization and wave vector of the excitation plane wave is along the x-axis and z-axis, respectively.

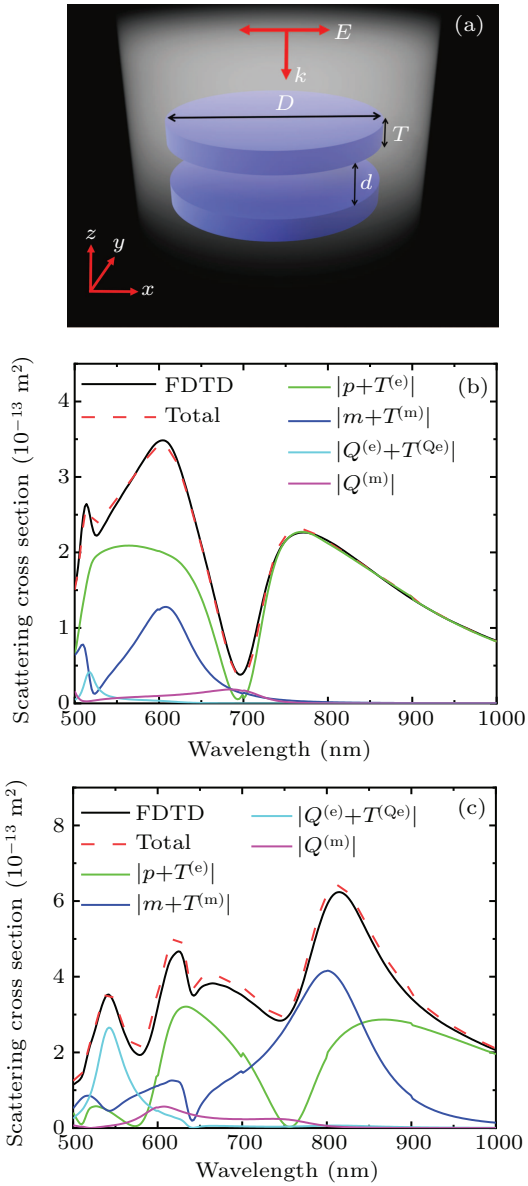


Fig. 1. (a) Schematic illustration of two stacked Si nanodisks with an x-polarized plane wave excitation. The distance between the nanodisks is d. The origin of the coordinate system is placed at the center of the structure. (b) and (c) The scattering spectrum of an individual Si nanodisk (b) and the stacked nanodisks (c). The contributions from different multipole modes are also shown. They are integrated ED and ETD mode ($|p+T^{(e)}|$), integrated MD and MTD mode ($|m+T^{(m)}|$), integrated EQ and ETQ mode ($|Q^{(e)}+T^{(Qe)}|$), and the magnetic quadrupole (MQ) mode ($|Q^{(m)}|$).

Crystalline Si is chosen as the material for the structure, and the dielectric constants are taken from Palik's book.[39] The index of the surrounding medium is 1. The simulations were carried out by using commercial finite-difference time-domain (FDTD) software (Lumerical FDTD). The Cartesian multipole decomposition method was used to calculate further the contribution of different multipole modes to the scattering spectrum. The Cartesian multipoles include ED, MD, electric quadrupole (EQ), magnetic quadrupole (MQ), ETD and MTD, where these vectors in Fig. 1 are denoted by P, m, $Q^{(e)}$, $Q^{(m)}$, $T^{(e)}$ and $T^{(m)}$, respectively. The diameter D and thickness T of each Si disk are 300 nm and 80 nm, respectively. The scattering spectrum of an individual disk is shown in Fig. 1(b). The sum of the contributions of different multipole modes is in good agreement with the results of the direct FDTD calculation of the scattering spectrum (Fig. 1(b)), which means that the contribution of higher-order modes can be ignored.

The dip on the scattering spectrum ($\sim$700 nm) of the individual disk is an electric anapole mode induced by the destructive interference of the ED and ETD responses. The scattering spectrum of the stacked Si nanodisks is shown in Fig. 1(c). There are two apparent dips at the wavelengths of $\lambda = 640$ nm and $\lambda = 760$ nm. The appearance of two dips indicates the strong coupling between the two nanodisks. Multipole decomposition results show that at the wavelengths of $\lambda = 760$ nm, the main contributions to the spectral responses are the integrated ED and ETD modes ($|p+T^{(e)}|$), and the spectral behavior is similar to the anapole mode of the individual disk. The dip at $\lambda = 64$ nm mainly comes from the integrated MD and MTD modes ($|m+T^{(m)}|$). In addition, there are also contributions of integrated EQ and ETQ modes ($|Q^{(e)}+T^{(Qe)}|$) and the magnetic quadrupole (MQ) mode ($|Q^{(m)}|$).

We calculated the electromagnetic near-field distributions to gain further insight into the electromagnetic interactions at the two dips of the scattering spectrum. Figures 2(a) and 2(b) show the electric field enhancement and direction of the upper and lower disks. The wavelength is $\lambda = 640$ nm, which corresponds to the first dip position of the scattering spectrum. The electric field loops appear on each disk, which correspond to the ETD moments. However, the two ETD moments show opposite directions, where the loops show opposite rotating directions. This corresponds to the anti-bonding hybridization of the two ETD moments, which is similar to the hybridizations of electric dipoles.[7] Figure 2(c) shows the electric field enhancement and directions on the $x = 0$ plane. The wavelength is also $\lambda = 640$ nm. The field distribution also confirms the existence of the ETD hybridization at this wavelength. Figures 2(d)–2(f) show the electric field enhancement and the field directions at the wavelength of $\lambda = 760$ nm, which is another dip of the scattering spectrum. The ETD moments can also be found on the disks, although they show the same direction, indicating bonding hybridization occurs. The bonding

hybridization of the ETD moments forms a new ETD moment of the dimer. This new ETD can interact with the ED moment of the dimer and induce an anapole mode of the dimer at $\lambda = 760$ nm.

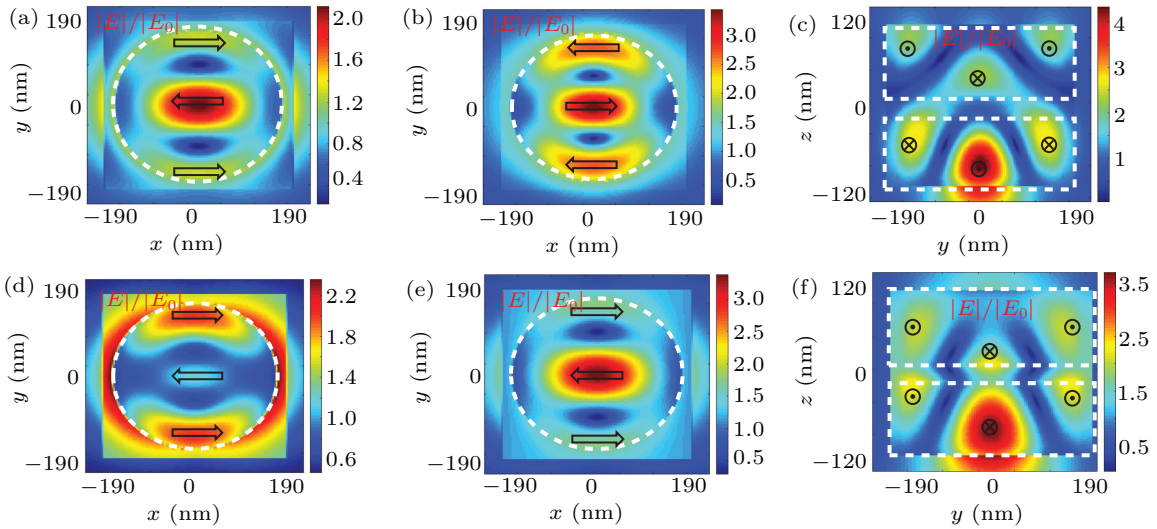


Fig. 2. Hybridization of the ETD modes. (a) and (b) Electric field enhancement of the upper (a) and lower (b) disks of the dimer structure. The wavelength is $\lambda = 640$ nm. The arrows show the electric field directions. (c) Electric field enhancement and directions on the $x = 0$ plane of the dimer structure at $\lambda = 640$ nm. (d) and (e) Electric field enhancement of the upper (d) and lower (e) disks of the dimer structure. The wavelength is $\lambda = 760$ nm. The arrows show the electric field directions. (f) Electric field enhancement and directions on the $x = 0$ plane at $\lambda = 760$ nm.

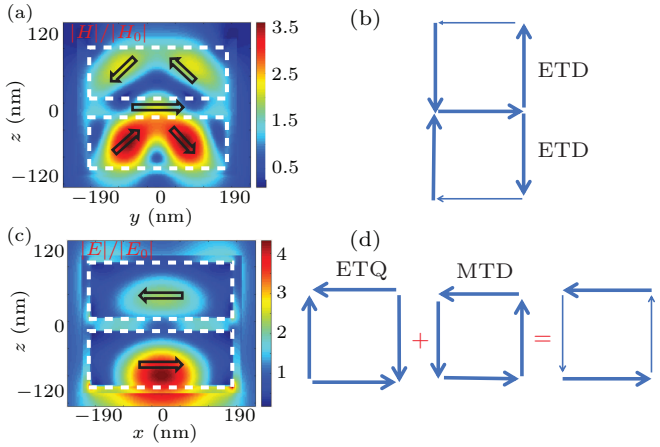


Fig. 3. (a) Magnetic field enhancements on the $x = 0$ plane of the disk dimer at $\lambda = 640$ nm. The arrows show the magnetic directions. (b) Schematic illustration of the MD moments associated with the formation of MTD. (c) Electric field enhancement and the field directions on the $y = 0$ plane at $\lambda = 640$ nm. (d) Schematic illustration of the ETD moments associated with the combined ETQ and MTD modes.

The dip feature at $\lambda = 640$ nm is mainly induced by the magnetic response, as shown in Fig. 1(c). This indicates that there may be a magnetic anapole mode here. This is confirmed by the magnetic field distribution on the $x = 0$ plane (Figs. 3(a) and 3(b)). Each disk shows two main MD moments with opposite directions, which is associated with the ETD response of the disk. There is another MD moment in between the two disks. These MD moments form an MTD response, where a similar situation can be found in other structures.[38] It is noted that the MD moments of the disks are associated with the anti-bonding hybridization of the ETD moments of the two disks. This MTD will destructively interfere with the original MD response of the dimer and induce the magnetic anapole resonance. In addition to the MTD response, the EQ part also shows a dip feature at $\lambda = 640$ nm (Fig. 1(d)). Nearfield distribution results show that this is closely related to MTD response (Figs. 3(c) and 3(d)). Each disk has an ETD moment, while MTD formation requires a closed loop of the ETD moments, implying there should also be an ETD moment between the disks to form a perfect MTD. However, this is not the case, as shown by Fig. 3(c). Thus, ETQ is also excited, and the combination of MTD and ETQ will cancel the ETD moment between the two disks.

The hybridizations of the disk's ETDs and the MTD response can be largely turned by varying the geometries of the dimer. Figure 4(a) shows the calculated scattering spectra with the surface distance d between the disks from 0 nm to 40 nm, where the other parameters are the same as that in Fig. 1. As the distance decreases, the hybridization of the ETDs becomes stronger. This change will induce redshift (blueshift) of the bonding (anti-bonding) dip. Similar phenomena have been well known in ED and MD systems.[10,40] As to the response dip feature, the stronger bonding response induces a more pronounced dip associated with the electric anapole mode. On the other hand, the stronger anti-bonding coupling reduces the MTD response and the corresponding dip feature associated with the magnetic anapole mode. We also consider the influence of thickness T on the ETD hybridization (Fig. 4(b)). It can be easily checked that the anapole mode of an individual disk redshifts with the thickness. Thus, both dips associated with the hybridized modes redshift with the thickness. The dip of the magnetic anapole mode becomes relatively weaker with the thickness T. This is because the MD mode of the dimer redshifts faster than MTD with T, and the multipole expansion calculations can confirm the overlapped part of the MD

mode becomes weaker.

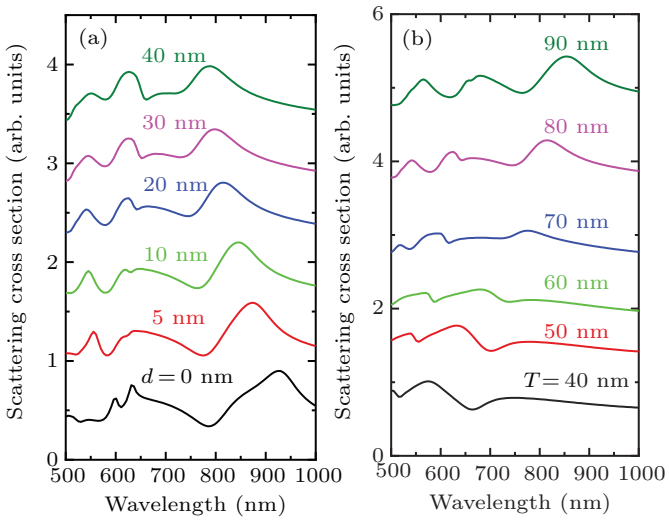


Fig. 4. (a) Scattering spectra of stacked disks with different surface distance d (0–40 nm). Each disk is the same as in Fig. 1. (b) Scattering spectra of stacked disks with different thickness T (60–90 nm). The radius of each disk is 150 nm, and the surface distance is 20 nm.

3. Conclusion and perspectives

In conclusion, we demonstrated that strong hybridizations of the ETD modes can occur in all-dielectric stacked disks. Each disk holds an electric anapole mode formed by combining an ED and an ETD mode. The anti-bonding hybridization of the ETD modes can form an MTD mode in the disk dimer. The MTD will cause interference with the dimer's magnetic dipole mode and form a magnetic anapole mode. We also performed multipole expansion and near-field distribution calculations to identify the electromagnetic responses. The MTD mode can be adjusted by changing the geometry of the disk dimer. The strong ETD hybridizations and the associated electromagnetic responses in simple dielectric nanostructures provide a rich optical manipulation platform for nanoscale electric and magnetic fields. They may also find applications in fields such as nanoantennas, metasurfaces and metamaterials.

Acknowledgements

Project supported by the National Natural Science Foundation of China (Grant Nos. 11704416 and 11704107), the Hunan Provincial Natural Science Foundation of China (Grant No. 2021JJ20076), and the Hubei Provincial Natural Science Foundation of China (Grant No. 2020CFB557).

References

[1] Genevet P, Capasso F, Aieta F, Khorasaninejad M and Devlin R 2017 *Optica* **4** 139
[2] Khorasaninejad M and Capasso F 2017 *Science* 358 eaam8100
[3] Kauranen M and Zayats A V 2012 *Nat. Photon.* **6** 737
[4] Koshelev K, Kruk S, Melik-Gaykazyan E, Choi J H, Bogdanov A, Park H G and Kivshar Y 2020 *Science* **367** 288
[5] Biagioni P, Huang J S and Hecht B 2012 *Rep. Prog. Phys.* **75** 024402
[6] Caldarola M, Albella P, Cortes E, Rahmani M, Roschuk T, Grinblat G, Oulton R F, Bragas A V and Maier S A 2015 *Nat. Commun.* **6** 7915
[7] Halas N J, Lal S, Chang W S, Link S and Nordlander P 2011 *Chem. Rev.* **111** 3913
[8] Kuznetsov A I, Miroshnichenko A E, Brongersma M L, Kivshar Y S and Luk'yanchuk B 2016 *Science* 354 aag2472
[9] Yang Z J, Jiang R B, Zhuo X L, Xie Y M, Wang J F and Lin H Q 2017 *Phys. Rep.* **701** 1
[10] Zywietz U, Schmidt M K, Evlyukhin A B, Reinhardt C, Aizpurua J and Chichkov B N 2015 *ACS Photon.* **2** 913
[11] Miroshnichenko A E and Kivshar Y S 2012 *Nano Lett.* **12** 6459
[12] Yan J H, Liu P, Lin Z Y, Wang H, Chen H J, Wang C X and Yang G W 2015 *ACS Nano* **9** 2968
[13] Cai D J, Huang Y H, Wang W J, Ji W B, Chen J D, Chen Z H and Liu S D 2015 *J. Phys. Chem. C* **119** 4252
[14] Baryshnikova K V, Smirnova D A, Luk'yanchuk B S and Kivshar Y S 2019 *Adv. Opt. Mater.* **7** 1801350
[15] Miroshnichenko A E, Evlyukhin A B, Yu Y F, Bakker R M, Chipouline A, Kuznetsov A I, Luk'yanchuk B, Chichkov B N and Kivshar Y S 2015 *Nat. Commun.* **6** 8069
[16] Koshelev K, Favraud G, Bogdanov A, Kivshar Y and Fratalocchi A 2019 *Nanophotonics* **8** 725
[17] Yang Y Q and Bozhevolnyi S I 2019 *Nanotechnology* **30** 204001
[18] Zanganeh E, Evlyukhin A, Miroshnichenko A, Song M, Nenasheva E and Kapitanova P 2021 *Phys. Rev. Lett.* **127** 096804
[19] Alaee R, Rockstuhl C and Fernandez-Corbaton I 2017 *Opt. Commun.* **407** 17
[20] Gurvitz E A, Ladutenko K S, Dergachev P A, Evlyukhin A B, Miroshnichenko A E and Shalin A S 2019 *Laser Photon. Rev.* **13** 1800266
[21] Deng Y H, Yang Z J, Hu M L, Du X J and He J 2021 *New J. Phys.* **23** 023004
[22] Yang Y Q, Zenin V A and Bozhevolnyi S I 2018 *ACS Photon.* **5** 1960
[23] Zhang Wu F, Li Q, Feng Q, Wu Y and Wu L 2020 *Opt. Express* **28** 570
[24] Baryshnikova K, Filonov D, Simovski C, Evlyukhin A, Kadochkin A, Nenasheva E, Ginzburg P and Shalin A S 2018 *Phys. Rev. B* **98** 165419
[25] Sabri L, Huan Q L, Liu N and Cunningham B 2019 *Opt. Express* **27** 7196
[26] Shibanuma T, Grinblat G, Albella P and Maier S A 2017 *Nano Lett.* **17** 2647
[27] Grinblat G, Li Y, Nielsen M P, Oulton R F and Maier S A 2017 *ACS Photon.* **4** 2144
[28] Grinblat G, Li Y, Nielsen M P, Oulton R F and Maier S A 2016 *Nano Lett.* **16** 4635
[29] Xu L, Rahmani M, Kamali K Z, Lamprianidis A, Ghirardini L, Sautter J, Camacho-Morales R, Chen H T, Parry M, Staude I, Zhang G Q, Neshev D and Miroshnichenko A E 2018 *Light Sci. Appl.* **7** 44
[30] Verre R, Baranov D G, Munkhbat B, Cuadra J, Kall M and Shegai T 2019 *Nat. Nanotechnol.* **14** 679
[31] Liu S D, Fan J L, Wang W J, Chen J D and Chen Z H 2018 *ACS Photon.* **5** 1628
[32] Du K, Li P, Gao K, Wang H, Yang Z Q, Zhang W D, Xiao F J, Chua S J and Mei T 2019 *J. Phys. Chem. Lett.* **10** 4699
[33] Thakkar N, Rea M T, Smith K C, Heylman K D, Quillin S C, Knapper K A, Horak E H, Masiello D J and Goldsmith R H 2017 *Nano Lett.* **17** 6927)
[34] Liu J N, Huang Q L, Liu K K, Singamaneni S and Cunningham B T 2017 *Nano Lett.* **17** 7569
[35] Wu P C, Liao C Y, Savinov V, Chung T L, Chen W T, Huang Y W, Wu P R, Chen Y H, Liu A Q, Zheludev N I and Tsai D P 2018 *ACS Nano* **12** 1920
[36] Luk'yanchuk B, Paniagua-Dominguez R, Kuznetsov A I, Miroshnichenko A E and Kivshar Y S 2017 *Phys. Rev. A* **95** 063820
[37] Li S Q and Crozier K B 2018 *Phys. Rev. B* **95** 245423
[38] Yang Z J, Deng Y H, Yu Y and He J 2020 *Nanoscale* **12** 10639
[39] Palik E D 1985 *Handbook of Optical Constants of Solids* (New York: Palik) pp. 547–570
[40] Prodan E, Radloff C, Halas N J and Nordlander P 2003 *Science* **302** 419